Observation of a new electronic state of CO perturbing W Π 1 (v = 1)

A. N. Heays, M. Eidelsberg, G. Stark, J. L. Lemaire, L. Gavilan, S. R. Federman, B. R. Lewis, J. R. Lyons, N. de Oliveira, and D. Joyeux

Citation: The Journal of Chemical Physics **141**, 144311 (2014); doi: 10.1063/1.4897326
View online: http://dx.doi.org/10.1063/1.4897326
View Table of Contents: http://scitation.aip.org/content/aip/journal/jcp/141/14?ver=pdfcov
Published by the AIP Publishing

Observation of a new electronic state of CO perturbing $W\,^1\Pi(v = 1)$

A. N. Heays,[1,a)] M. Eidelsberg,[2] G. Stark,[3] J. L. Lemaire,[2] L. Gavilan,[2,b)] S. R. Federman,[4] B. R. Lewis,[5] J. R. Lyons,[6] N. de Oliveira,[7] and D. Joyeux[7]

[1]*Leiden Observatory, Leiden University, P. O. Box 9513, 2300 RA Leiden, The Netherlands*
[2]*Observatoire de Paris, LERMA and UMR 8112 du CNRS, 5 place Jules Janssen, 92195 Meudon, France*
[3]*Department of Physics, Wellesley College, Wellesley, Massachusetts 02481, USA*
[4]*Department of Physics and Astronomy, University of Toledo, Toledo, Ohio 43606, USA*
[5]*Research School of Physics and Engineering, The Australian National University, ACT 0200 Canberra, Australia*
[6]*School of Earth and Space Exploration, Arizona State University, 781 S. Terrace Rd, Tempe, Arizona 85281, USA*
[7]*Synchrotron SOLEIL, Orme de Merisiers, St. Aubin, BP 48, 91192 Gif sur Yvette Cedex, France*

(Received 25 July 2014; accepted 25 September 2014; published online 14 October 2014)

We observe photoabsorption of the $W(1) \leftarrow X(0)$ band in five carbon monoxide isotopologues with a vacuum-ultraviolet Fourier-transform spectrometer and a synchrotron radiation source. We deduce transition energies, integrated cross sections, and natural linewidths of the observed rotational transitions and find a perturbation affecting these. Following a deperturbation analysis of all five isotopologues, the perturbing state is assigned to the $v = 0$ level of a previously unobserved $^1\Pi$ state predicted by *ab initio* calculations to occur with the correct symmetry and equilibrium internuclear distance. We label this new state $E''\,^1\Pi$. Both of the interacting levels $W(1)$ and $E''(0)$ are predissociated, leading to dramatic interference effects in their corresponding linewidths. © *2014 AIP Publishing LLC*. [http://dx.doi.org/10.1063/1.4897326]

I. INTRODUCTION

This paper is part of a series studying the photoabsorption and photodissociation of carbon monoxide (CO) at vacuum-ultraviolet (VUV) wavelengths.[1–5] These phenomena are of relevance to astrophysics because CO is the second most abundant molecule in the Universe (following H_2) and chemically stable, and therefore provides a sink of C and O atoms, limiting the formation of larger C- and O-bearing molecules.[6,7] The liberation of CO's constituent atoms is principally achieved by VUV photodissociation in regions exposed to radiation having a wavelength shorter than 120 nm. High-resolution absolutely calibrated photoabsorption measurements are needed for quantifying this, and are most useful after a detailed reduction to absorption-line wavelengths, oscillator strengths (*f*-values), and predissociation linewidths (or rates). This detailed information enables translation of the experimental spectra into model cross sections for astrophysical use.[6,8] A related phenomenon is isotopologue-dependent self-shielding, whereby, even small differences between isotopologues in the highly structured CO spectrum can lead to isotopic ratios of C and O atoms deviating from their elemental abundances. This isotopic fractionation can be propagated further in the astrophysical photochemistry networks.[6,9,10]

More fundamentally, we seek to study the excited states of CO and their many perturbations in detail. These consist of photoabsorbing mutually interactive $^1\Pi$ and $^1\Sigma^+$ states of Rydberg and valence type,[2,11–13] as well as perturbing $^3\Pi$ states connected to the singlet manifold by spin-orbit interaction.[14–16] Much of the known vibrational, rotational, and isotopological dependence of CO predissociation has never been explained but likely arises from the interplay of all of these excited states, including those that only appear weakly in photoabsorption spectra.

The subject of this paper is the $v = 1$ level of the $W\,^1\Pi$ state, its photoexcitation, and its perturbation by a previously unobserved level. We consider five isotopologues: $^{12}C^{16}O$, $^{12}C^{17}O$, $^{12}C^{18}O$, $^{13}C^{16}O$, and $^{13}C^{18}O$. The $W\,^1\Pi$ state consists of a $3s\sigma$ Rydberg electron built on the $A^2\Pi$ excited state of CO^+ and leads to several prominent bands in the 90–100 nm region of the ground-state absorption spectrum. Recent measurements of the $W(v') - X(0)$ absorption bands with $v' = 0 - 4$ were performed by Eidelsberg *et al.*[1,4] for the $^{12}C^{16}O$, $^{13}C^{16}O$, and $^{12}C^{18}O$ isotopologues, giving rotationally-resolved *f*-values and linewidths. These detailed measurements revealed large rotational dependences in these quantities for the majority of bands. The $W(1) \leftarrow X(0)$ band, in particular, has been studied previously in absorption,[17–23] with most experiments focussing on $^{12}C^{16}O$. Further complications in the $^{12}C^{16}O$ $W(1) \leftarrow X(0)$ photodissociation spectrum were identified by Gao *et al.*[24] by means of VUV laser excitation of CO and velocity discrimination of the atomic-C dissociation product. They determined that the lowest rotational levels of $W(1)$ decay via two channels, yielding both $C(^1D) + O(^3P)$ and $C(^3P) + O(^3P)$ dissociation products.

A comprehensive *ab initio* calculation of CO's excited valence states was performed by O'Neil and Schaefer[25] for many classes of electronic symmetry and more recently by Guberman.[26] Vázquez *et al.*[27] further included molecular orbitals representing Rydberg states in a calculation of $^1\Sigma^+$ and $^{1,3}\Pi$ states. Some of the experimentally important

a)Electronic mail: heays@strw.leidenuniv.nl
b)Now at IAS (Institut d'Astrophysique Spatiale), Orsay, France.

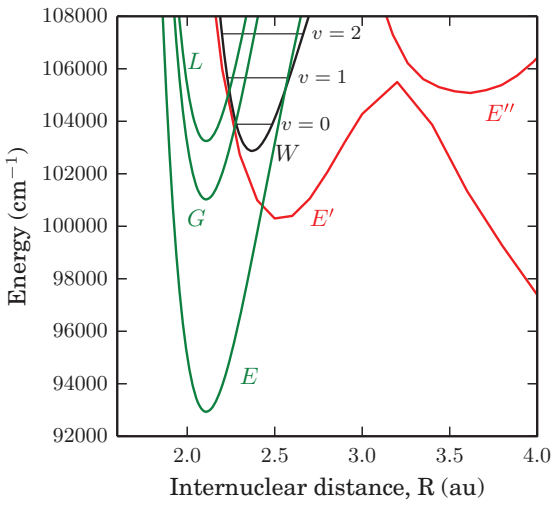

FIG. 1. Potential-energy curves of $^1\Pi$ states of CO relative to the ground-state potential minimum. *Red*: Adiabatic valence-state curves calculated *ab initio* by Guberman,[26] reproduced from his Table 4 and Fig. 2. *Black and green*: Experimentally deduced diabatic curves for $W\,^1\Pi$ and some further Rydberg states of Lefebvre-Brion and Eidelsberg,[2] also showing experimental energies for the first three vibrational levels of $W\,^1\Pi$ for $^{12}C^{16}O$.

adiabatic states calculated *ab initio* have been treated diabatically. Lefebvre-Brion and Lewis[13] deduced approximate potential-energy curves for $W\,^1\Pi$ and its curve crossing with the $E'\,^1\Pi$ valence state. Lefebvre-Brion and Eidelsberg[2] quantitatively refined the W and E' diabatic potential-energy curves (as well as several other $^1\Pi$ Rydberg states) and inferred a large electronic interaction mixing the two states. A combination of valence states (calculated *ab initio*) and diabatic Rydberg states of relevance to this study are plotted in Fig. 1.

II. EXPERIMENTAL AND ANALYSIS METHODS

All spectra were recorded using the Fourier-transform spectrometer permanently attached to the DESIRS beamline of the SOLEIL synchrotron. Technical details of this unique wavefront-division interferometric spectrometer and the undulator insertion element responsible for generating VUV photons at the beamline may be found elsewhere.[28–30]

The best achievable spectral resolution of the instrument is 0.07 cm^{-1} FWHM but all absorption lines in our spectra are much broader than this and resolution settings between 0.22 and 0.65 cm^{-1} FWHM were used. The sample gases were observed free-flowing through a differentially pumped cell. This windowless setup was required for the transmission of VUV radiation through the apparatus but prevented an absolute determination of the sample column densities. The column density was instead calibrated by recording the $B\,^1\Sigma^+(v = 0) \leftarrow X(0)$ absorption band, for which an absolute f-value is known, under identical conditions. The calibrating f-value and its 7% 1σ-uncertainty is the average of two independent experiments[31,32]

$$f\text{-value } B(0) - X(0) = 0.0065 \pm 0.0005. \qquad (1)$$

Additional effects in our experiment are estimated to increase the systematic uncertainty of f-values deduced from each spectrum to 10%. These effects arise from small fluctuations in the pressure of the absorbing CO during the course of some measurements and mechanical vibrations affecting the alignment of the synchrotron beam and the interferometer, with further details discussed elsewhere.[4,5,33]

Additional information regarding the absorption cell, isotopically purified gas samples, and column density calibration are given in our previous publications.[1,4,5]

Spectra were recorded at multiple column densities between 8×10^{14} and 3×10^{16} cm^{-2} in order to observe both weak and strong lines with approximately unity peak optical depths. Most spectra were recorded at room temperature (295 K) but some others were taken while cooling with liquid N_2 to 90 ± 5 K in order to reduce the number of excited rotational transitions and avoid spectral blending. The lower temperature was diagnosed from a recorded rotational profile of the well-resolved $W(0) \leftarrow X(0)$ band.

The recorded absorption spectra were reconstructed by a model requiring the positions, integrated cross sections, and natural linewidths of all observed absorption lines. This was then compared point-wise with the experimental scans and iteratively optimised. The model generates a summed cross section by adopting Voigt profiles for each line, composed of Lorentzian natural and Gaussian Doppler broadening. The summed cross section was converted into a transmission spectrum according to the Beer-Lambert formula and convolved with a sinc function to reproduce the instrumental broadening of the spectrometer. Further details of this analysis procedure have been given previously.[4,5,33]

The integrated cross section deduced for each $W(v' = 1, J') \leftarrow X(v'' = 0, J'')$ line was converted into a temperature-independent band f-value by factoring the fractional excitation of each J'' rotational level assuming a thermally populated ground state, a $2J'' + 1$ ground-state degeneracy factor, and appropriate Hönl-London rotational linestrength factors.[33,34] The levels observed here are all completely dissociative and the observed natural linewidths, Γ, are directly related to the excited-state predissociation lifetime, $\tau = 1/2\pi c\Gamma$, where c is the speed of light. The contribution of radiative decay to the natural linewidths is negligible for $W(1)$.

The wavenumber scales of our spectra were absolutely calibrated by comparing the positions of lines from a contaminating N_2 band, $c_4'\,^1\Sigma_u^+(v' = 0) \leftarrow X\,^1\Sigma_g^+(v'' = 0)$, with an absolute reference experiment.[35] This calibration is estimated to be accurate within 0.015 cm^{-1}. The wavenumber and linewidth uncertainties of $W(1) \leftarrow X(0)$ transitions deduced from our spectra depend very much on their degree of blending, but in many cases are below 0.1 cm^{-1}. The observed transition wavenumbers were converted to excited-state term values using the ground-state energy-level parameterisation of Coxon and Hajigeorgiou.[36] Term values are given relative to the ground-state equilibrium energy unless stated otherwise because of the multiple isotopologues considered in this study.

The 10% systematic uncertainty of our column-density calibration dominates the uncertainty of our $W(1) \leftarrow X(0)$ f-values for the best-resolved absorption lines. For weak and blended lines, the fitting uncertainty is more important. All

discussed and plotted uncertainties consist of 1σ fitting errors only, unless otherwise specified.

III. RESULTS

Spectroscopic analyses were made of the $W(1) \leftarrow X(0)$ absorption band at 95.6 nm for all five isotopologues. General remarks are presented here and Secs. III A–III E discuss isotopologue-dependent details.

The observed absorption bands are plotted in Figs. 2–4. The rotational lines of all isotopologues are significantly blended and predissociation broadened, but a first clue to their assignment arises from the small number of apparently narrow well-resolved lines. For example, the $P(9)$, $Q(8)$, and $R(7)$ lines in $^{12}C^{18}O$ are clearly identifiable in Fig. 3 and conform to their expected combination differences. Transition wavenumbers, integrated absorption cross sections, and natural full-width at half-maximum (FWHM) linewidths were assigned to all observed rotational lines beginning from such easily assigned features. These data are summarised in Figs. 5–8; and given in full in the supplementary material.[37] Not all experimental line parameters could be determined independently and some interpolations and assumptions were necessary. For example, the Λ-doubling of $W(1)$ *e*- and *f*-parity levels is very small (<0.2 cm^{-1} in all cases) and was frequently neglected when fitting broad and blended lines.

All isotopologues exhibit an apparent perturbation of $W^1\Pi$ term values due to another state of lower rotational constant, hereafter labelled $E''(0)$ (see Sec. IV). For $^{12}C^{16}O$, this occurs between $J = 5$ and 6, for $^{12}C^{17}O$ between $J = 6$ and 7; and for $^{12}C^{18}O$, $^{13}C^{16}O$, and $^{13}C^{18}O$ between $J = 7$ and 8. The resultant deflection of the $W(1)$ term series is apparent in Fig. 5 as sudden jumps in otherwise smooth progressions. Accompanying these level crossings are natural-linewidth variations, shown in Fig. 7, which follow a common pattern for all isotopologues: lines are suddenly narrower after the crossing point but continue to broaden (apart from the case of $^{13}C^{18}O$).

The lines of $W(1) \leftarrow X(0)$ nearest its crossing with the perturber state are weakened, with band *f*-values shown in

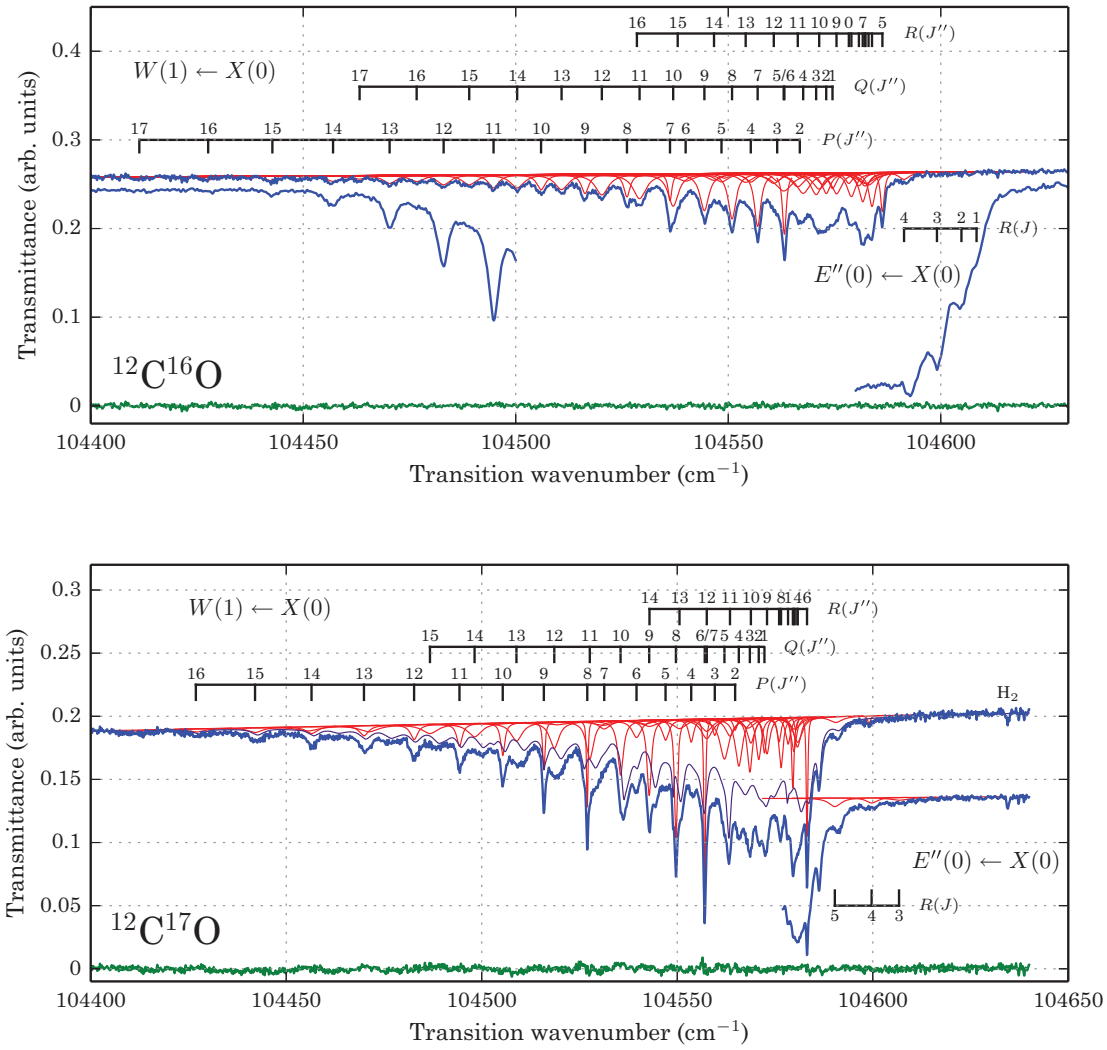

FIG. 2. Absorption spectra showing $W(1) \leftarrow X(0)$ and transitions to the perturber state, labelled $E''(0) \leftarrow X(0)$, for the $^{12}C^{16}O$ and $^{12}C^{17}O$ isotopologues. *Upper blue lines*: Lower-pressure room-temperature spectra. *Lower blue lines*: Higher-pressure liquid-N_2-cooled spectra. *Red lines*: Model profiles of individual rotational transitions. *Green lines*: Residual errors of fits to the low pressure spectra. *Thin indigo line in* $^{12}C^{17}O$: The contributing absorption of contaminating $^{12}C^{16}O$ and $^{12}C^{18}O$ (sample composition: $^{12}C^{16}O$:$^{12}C^{17}O$:$^{12}C^{18}O$=1: 0.85: 0.20).

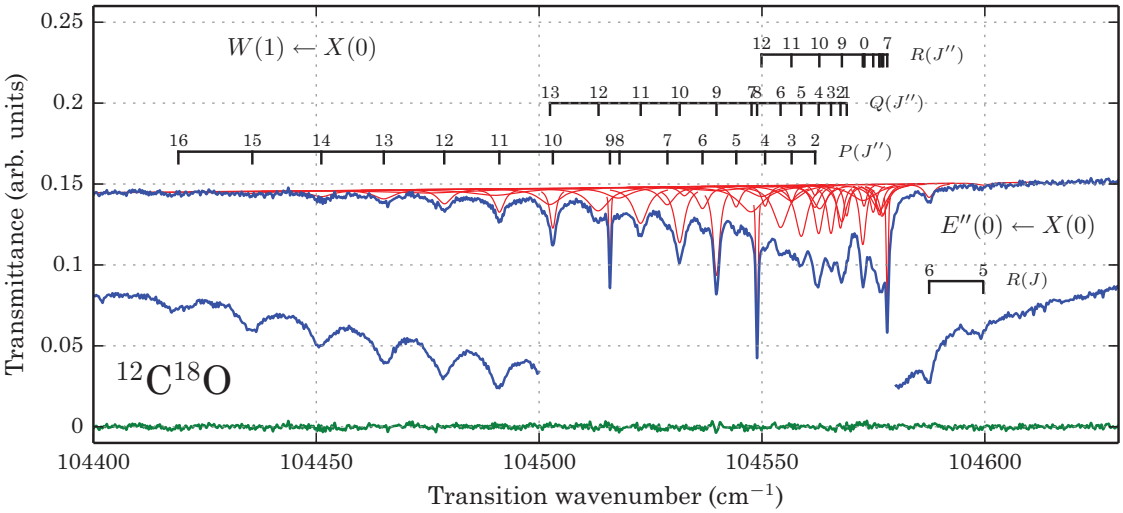

FIG. 3. Absorption spectra showing $W(1) \leftarrow X(0)$ and transitions to the perturber state, labelled $E''(0) \leftarrow X(0)$, for the $^{12}C^{18}O$ isotopologue. *Upper blue line*: Lower-pressure room-temperature spectrum. *Lower blue line*: Higher-pressure liquid-N_2-cooled spectrum. *Red lines*: Model profiles of individual rotational transitions. *Green line*: Residual errors of the fit to the low pressure spectrum.

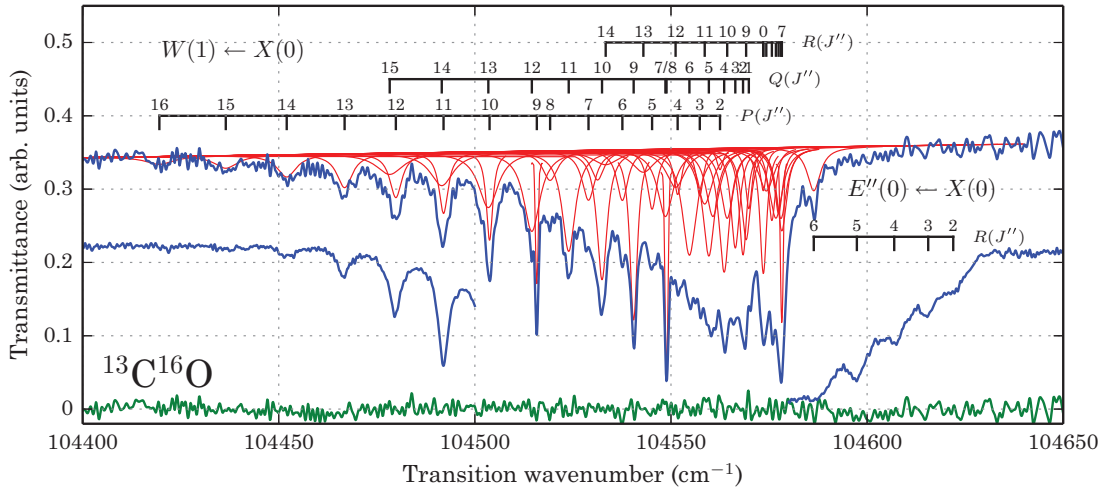

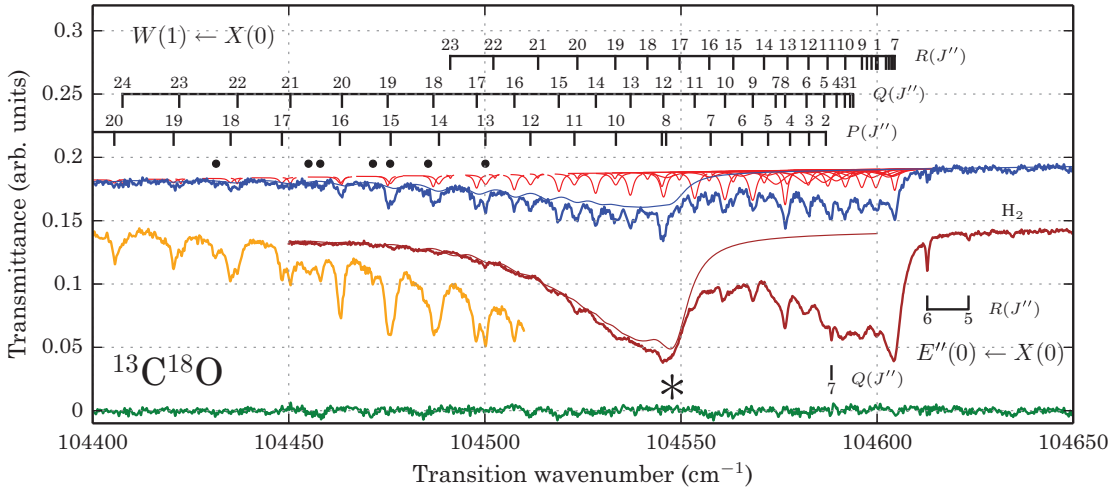

FIG. 4. Absorption spectra showing $W(1) \leftarrow X(0)$ and transitions to the perturber state, labelled $E''(0) \leftarrow X(0)$, for the $^{13}C^{16}O$ and $^{13}C^{18}O$ isotopologues. The peak of an additional broad feature overlapping $W(1) \leftarrow X(0)$ in $^{13}C^{18}O$ is indicated with an asterisk. *Upper blue lines*: Lower-pressure room-temperature spectra. *Lower blue line in* $^{13}C^{18}O$: Higher-pressure liquid-N_2-cooled spectrum. *Red lines*: Model profiles of individual rotational transitions. *Green lines*: Residual errors of fits to the low pressure spectra. *Brown line in* $^{13}C^{18}O$: Liquid-N_2 cooled spectrum. *Orange line in* $^{13}C^{18}O$: Higher-pressure room-temperature spectrum. *Thin blue and brown lines in* $^{13}C^{18}O$: Model band profiles fit to an additional broad feature. *Filled circles*: Further overlapping lines in $^{13}C^{18}O$ of unknown origin.

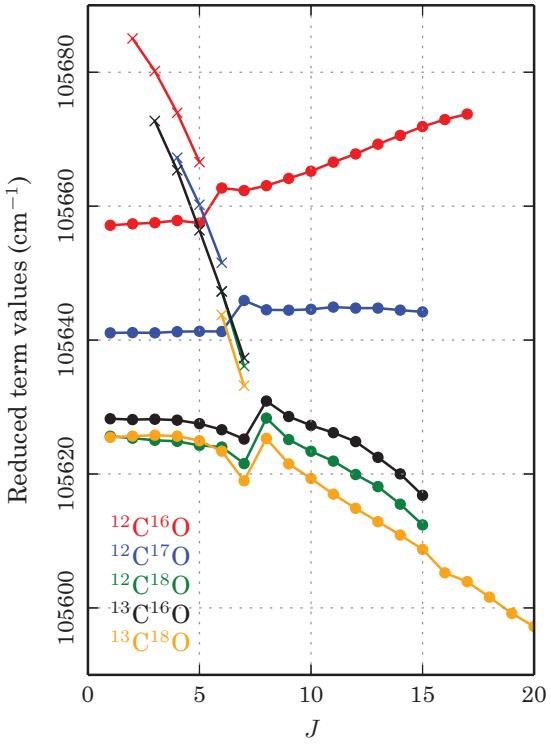

FIG. 5. Term values of $W(1)$ (*circles*) and the perturber state $E''(0)$ (*crosses*) for all isotopologues, reduced by the subtraction of a linear term: 1.5 cm^{-1} $J(J+1)$, and plotted relative to the ground state equilibrium energy of Coxon and Hajigeorgiou.[36]

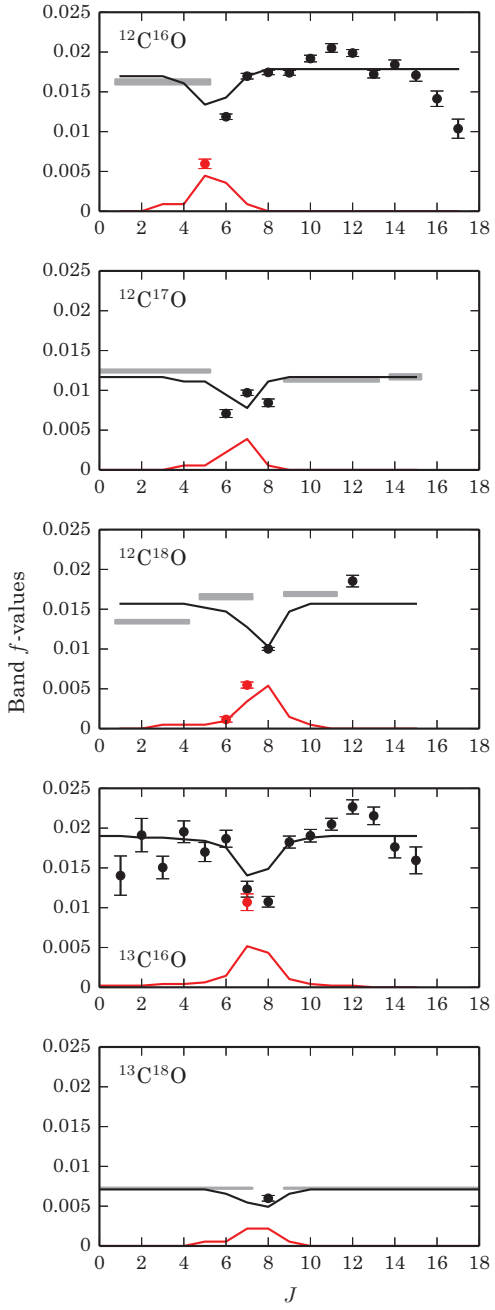

FIG. 6. Band f-values of the observed $W(1) \leftarrow X(0)$ transitions (*black*) and the perturber state (*red*) for all isotopologues, indexed by upper state rotational level J. *Error bars, circles*: Experimental data with 1σ uncertainties. *Filled grey regions*: Each region is fitted to a J-independent f-value with thickness indicating a 1σ fitting uncertainty. *Solid curves*: f-values calculated from the two-state mixing model.

Fig. 6. Extra lines appear at energies above the bandhead of $W(1) \leftarrow X(0)$ for all isotopologues. Assuming these to be borrowing strength from $W(1) \leftarrow X(0)$, they are assigned to the R-branch of the perturbing state with the strongest of these corresponding to the same J as the most weakened $W(1) \leftarrow X(0)$ lines. No perturbing rotational transitions are observed after the crossing point with $W(1)$ even though some higher-J $W(1)$ transitions are also evidently weakened in intensity. This non-appearance would be explained if the perturbing-state levels have increased natural linewidths after the crossing point.

The band f-values for some $W(1) \leftarrow X(0)$ transitions were assumed constant over short J-ranges, and the natural linewidths sometimes fitted to piecewise sections linearly dependent on $J(J+1)$. This was necessary to fit heavily blended features and the affected subsets of J are indicated in Figs. 6 and 7. The majority of Λ-doubling effects which distinguish between e- and f-parity excited levels were not resolved in our experiment. That is, an additional assumption was made adopting a common upper-state band f-value and linewidth for P-, Q-, and R-branch transitions exciting a common $W(1)$ rotational level. Common excited-state term values were also assumed, with some exceptions listed in the supplementary material.[37]

A. ^{12}C^{16}O

Two recorded absorption spectra showing $W(1) \leftarrow X(0)$ in ^{12}C^{16}O are plotted in Fig. 2. One of these is at room temperature and another scan was recorded with a liquid-N_2 cooled CO sample at approximately 10 times higher column density. With the latter settings, most rotational lines of $W(1) \leftarrow X(0)$ are completely absorbed but several further transitions to the perturber state above the $W(1) \leftarrow X(0)$ bandhead become visible. It was not possible to determine accurate integrated cross sections for these extra lines because of their blending with the $W(1) \leftarrow X(0)$ bandhead.

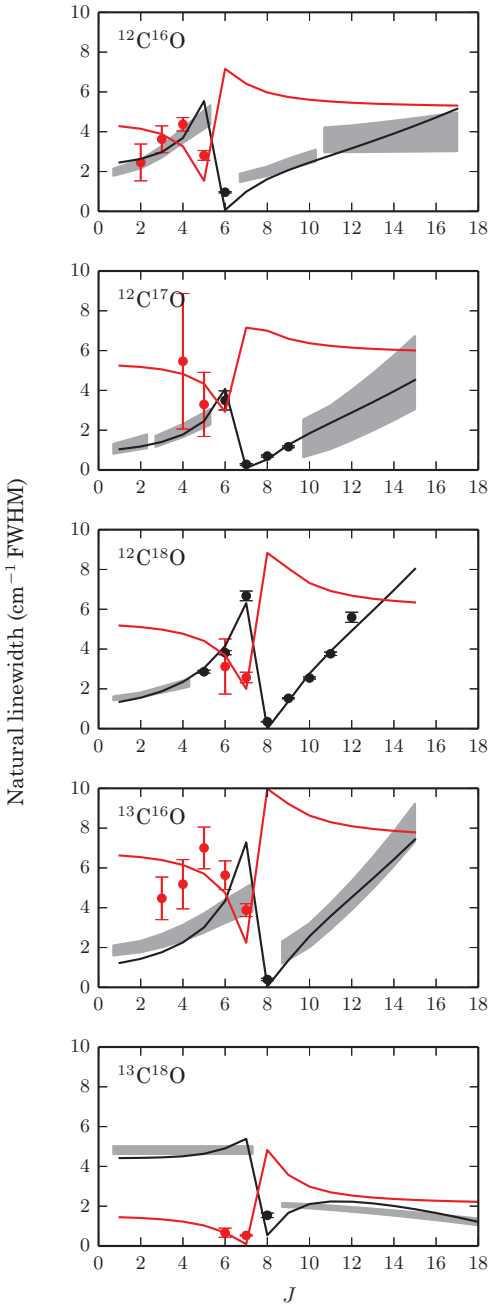

FIG. 7. Natural linewidths of the observed $W(1)$ (*black*) and $E''(0)$ levels (*red*) for all isotopologues, indexed by upper-state rotational level J. *Error bars, circles*: Experimental data with 1σ uncertainties. *Thick grey curves*: Short sections of linewidths fitted to assumed linear dependences in terms of $J(J+1)$ with thickness indicating a 1σ fitting uncertainty. *Solid curves*: Widths calculated from the two-state mixing model.

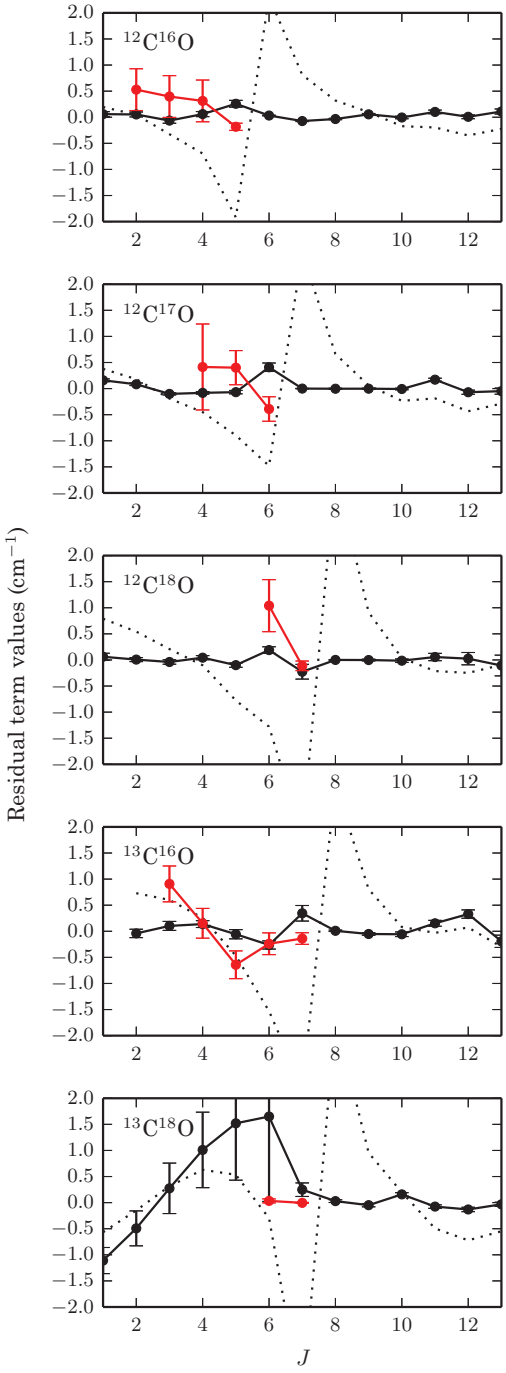

FIG. 8. Residual errors following the deperturbation of the $W(1)$ *(black)* and $E''(0)$ *(red)* rotational term values. Also shown is the residual of a fit to $W(1)$ term values neglecting their interaction with $E''(0)$ *(dotted lines)*.

B. $^{12}C^{17}O$

The analysis of $W(1) \leftarrow X(0)$ spectra obtained from our purified sample of $^{12}C^{17}O$ was hampered by its high degree of contamination from other isotopologues. A mixing ratio, $^{12}C^{17}O : {}^{12}C^{16}O : {}^{12}C^{18}O = 1 : 0.85 : 0.20$, was determined from an analysis of the $B\,^1\Sigma^+(0) \leftarrow X(0)$ band which is not predissociation broadened, allowing for easy discrimination of isotopologic lines, and has a mass-independent f-value.[5] A spectrum recorded at room temperature is shown in Fig. 2 along with the assignments of $^{12}C^{17}O$ absorption lines, and a partial model indicating the contribution of $^{12}C^{16}O$ and $^{12}C^{18}O$ to the observed absorption. The line positions, widths, and relative cross sections of the contaminating $^{12}C^{16}O$ and $^{12}C^{18}O$ lines are identical to those determined in Secs. III A and III C, and were uniformly scaled in strength to make a best fit while analysing $^{12}C^{17}O$. Three extra lines are apparent in a higher column density spectrum of $^{12}C^{17}O$ above the $W(1) \leftarrow X(0)$ bandhead, and are assigned to $R(3)$, $R(4)$, and $R(5)$ transitions.

C. $^{12}C^{18}O$

The $W(1) \leftarrow X(0)$ band in $^{12}C^{18}O$, plotted in Fig. 3, resembles the case of $^{12}C^{16}O$ except that the level crossing with the perturber state occurs between $J = 7$ and 8. Also, the observed $^{12}C^{18}O$ linewidths after the crossing are somewhat broader. There are two predissociation-broadened extra lines above the $W(1) \leftarrow X(0)$ bandhead which are more evident in the recorded spectrum with higher column density.

D. $^{13}C^{16}O$

The widths of the mostly blended lines of $W(1) \leftarrow X(0)$ in $^{13}C^{16}O$ were assumed to follow linear $J'(J' + 1)$ dependences over the observed ranges above and below $J' = 8$. The narrow transitions leading to $J' = 8$ were fit to a single common linewidth. This band is accompanied by five extra lines appearing above its head. One of these, the $R(6)$ line, is sufficiently strong that its f-value and width could be quantified in a lower-pressure scan. The widths of the other extra lines were estimated from a very high-pressure scan recorded with the aid of liquid-N_2 cooling.

E. $^{13}C^{18}O$

Three absorption spectra showing $W(1) \leftarrow X(0)$ in $^{13}C^{18}O$ are plotted in Fig. 4: at room temperature (295 K), liquid-N_2 cooled (90 K), and at room temperature but with approximately 5 times greater column density. The $R(7)$, $Q(8)$, and $P(9)$ lines are identifiable in the low column density measurement as peaks in the optical depth, due to their reduced width. The remainder of the band is heavily overlapped and obscured, and the assumption of constant or linear $J(J + 1)$ dependences for the fitted f-values and linewidths was adopted, as indicated by polynomial fits in Figs. 6 and 7.

For this isotopologue, the perturbing state crosses $W(1)$ between $J = 7$ and 8 according to the term values deflections evident in Fig. 5. Two extra lines appear above the $W(1)$ bandhead and are assigned to $R(5)$ and $R(6)$ transitions. Another extra line is observed in the liquid-N_2 cooled spectrum and is assigned to a $Q(7)$ transition of the perturber, with its energy separation from the $R(6)$ line matching the expected combination difference assuming no Λ-doubling of the excited level.

There is a predissociation-broadened red-degraded feature overlapping the higher rotational lines of $W(1) \leftarrow X(0)$ and which is particularly apparent in the liquid-N_2 cooled spectrum. Its peak absorption is marked with an asterisk in Fig. 4. The profile of this feature was fit to a $^1\Pi \leftarrow X(0)$ band with excited-state spectroscopic parameters $T_0 = 104545\ \mathrm{cm}^{-1}$ and $B_v = 1.2\,\mathrm{cm}^{-1}$, and a J-independent f-value and natural linewidth, 0.01 and 8 cm^{-1} FWHM, respectively. These fitted parameters are highly model dependent but work reasonably well for both low and high temperature spectra. Attempts to fit this band as a $^1\Sigma^+ \leftarrow {}^1\Sigma^+$ transition were less satisfactory. The identity of this band is unknown but a possible candidate is the $v = 5$ level of the $E'\,^1\Pi$ state, which was predicted in an experimentally based model of interacting Rydberg and valence states to have $T_0 = 104580\,\mathrm{cm}^{-1}$ and $B_v = 1.09\ \mathrm{cm}^{-1}$ in $^{13}C^{18}O$.[2] Identifying similar levels in the other CO isotopologues may help to confirm this assignment.

A higher-pressure room temperature scan allowed for the observation of $W(1) \leftarrow X(0)$ transitions out to $J = 24$. This scan also revealed further extra lines appearing below $104500\ \mathrm{cm}^{-1}$, indicated in Fig. 4 by filled circles. The source of these extra lines could not be determined.

Finally, there is an additional perturbation of $W(1)$ energy levels between $J = 15$ and 16 appearing as a $1\ \mathrm{cm}^{-1}$ deflection of the term values shown in Fig. 5. The cause of this perturbation could not be determined but it affects both e- and f-parity term values.

IV. DEPERTURBATION OF ENERGY LEVELS

The interaction between $W(1)$ and the perturbing state affects the P, R, and Q branches of $W(1)$ equally and is therefore parity independent. Additionally, the perturbation only appears once in the rotational progressions of each isotopologue, suggesting a state of singlet multiplicity. The symmetry of the perturbing state is then likely to be $^1\Pi$, which is consistent with our $E''\,^1\Pi$ assignment, and its interaction with $W(1)$ to be of an homogeneous electronic type and independent of J.

For each isotopologue, a simple two-level deperturbation was made of the observed $W(1)$ and perturber term values. For this a J-dependent series of matrices,

$$\begin{bmatrix} T_W(J) & H_{WE''} \\ H_{WE''} & T_{E''}(J) \end{bmatrix}, \tag{2}$$

was repeatedly diagonalised until their eigenvalues best matched the experimental term values. Five adjustable parameters were optimised in this way which describe the deperturbed term series,

$$T_W(J) = T_W + B_W J(J+1) - D_W\,[J(J+1)]^2 \tag{3}$$

and

$$T_{E''}(J) = T_{E''} + B_{E''} J(J+1), \tag{4}$$

and a sixth parameter was used to simulate a homogeneous electronic perturbation mixing the two levels, $H_{WE''}$. The fitted parameters and their uncertainties are given in Table I and the residual errors of the fitted term values are plotted in Fig. 8.

The reduced-mass, μ, dependence of the deperturbed molecular parameters for $W(1)$ and the perturbing state may be compared with their expected first-order behaviour.[38] That is,

$$x = \frac{B_v[^A\mathrm{C}^B\mathrm{O}]\mu[^A\mathrm{C}^B\mathrm{O}]}{B_v[^{12}\mathrm{C}^{16}\mathrm{O}]\mu[^{12}\mathrm{C}^{16}\mathrm{O}]} \simeq 1 \tag{5}$$

and

$$\frac{\omega_e[^A\mathrm{C}^B\mathrm{O}]}{\omega_e[^{12}\mathrm{C}^{16}\mathrm{O}]} = \sqrt{\frac{\mu[^{12}\mathrm{C}^{16}\mathrm{O}]}{\mu[^A\mathrm{C}^B\mathrm{O}]}}. \tag{6}$$

TABLE I. Deperturbed molecular parameters of $W(1)$ and its perturbing level.[a]

			$W(1)$					Perturber, $E''(0)$				
	μ[b]	T_X[c]	T_W[d]	B_W	D_W	x[e]	y[f]	$T_{E''}$[d]	$B_{E''}$	x[e]	y[g]	$H_{WE''}$
$^{12}C^{16}O$	6.86	1081.78	105 657.52(9)	1.575(2)	$6.3(7) \times 10^{-5}$	1	−0.13	105 688.8(5)	0.69(2)	1	0.2	4.2(1)
$^{12}C^{17}O$	7.03	1068.03	105 641.28(7)	1.539(2)	$1.1(1) \times 10^{-4}$	1.003(2)	0.21	105 681(3)	0.77(6)	1.2(1)	−3.1	4.1(2)
$^{12}C^{18}O$	7.20	1055.72	105 626.09(6)	1.487(2)	$1.8(1) \times 10^{-4}$	0.992(2)	−0.15	105 679(2)	0.69(3)	1.06(5)	−0.8	5.7(1)
$^{13}C^{16}O$	7.17	1057.73	105 628.8(2)	1.501(3)	$2.0(2) \times 10^{-4}$	0.997(3)	0.16	105 681.2(7)	0.66(2)	1.01(4)	0.9	5.6(2)
$^{13}C^{18}O$	7.55	1031.05	105 627.6(4)	1.409(5)	$5(2) \times 10^{-5}$	0.985(4)	31	105 678.7(6)	0.62(1)	0.99(4)	7.6	6.4(2)

[a]All parameters in cm^{-1} and 1σ uncertainties are shown in parentheses in units of the least significant figure.
[b]Reduced mass (amu).
[c]Ground-state zero-point energy from the constants of Coxon and Hajigeorgiou.[36]
[d]Relative to the ground-state equilibrium energy.
[e]From Eq. (5).
[f]From Eq. (8), following a minimisation of parameters excluding $^{13}C^{18}O$ giving $T_e = 104\,357(4)$ cm^{-1} and $\omega_e[^{12}C^{16}O](v+\frac{1}{2}) = 1300(4)$ cm^{-1}.
[g]From Eq. (8), following a minimisation of parameters excluding $^{13}C^{18}O$ giving $T_e = 105\,318(39)$ cm^{-1} and $\omega_e[^{12}C^{16}O](v+\frac{1}{2}) = 370(40)$ cm^{-1}.

Here, ω_e describes the vibrational energy spacing of a harmonic oscillator with energy levels

$$T_v[^A C^B O] = T_e + \omega_e[^A C^B O]\left(v + \frac{1}{2}\right). \tag{7}$$

Then, the quantity

$$T_v[^A C^B O] - T_e - \sqrt{\frac{\mu[^{12}C^{16}O]}{\mu[^A C^B O]}}\omega_e[^{12}C^{16}O]\left(v + \frac{1}{2}\right) = y \tag{8}$$

should be zero for all isotopologues.

The calculated values of x and y from Eqs. (5) and (8) are listed in Table I and are generally close to 1 and 0, respectively, apart from the case of $^{13}C^{18}O$. The deviations from the expected mass scaling of the perturber state in all other isotopologues are consistent with the experimental uncertainties of the deduced x parameters and the term values from which y is calculated. This observation supports the rotational assignments of perturbing-state lines which were made for the most part without the benefit of confirming combination differences. The small range of isotope shifts deduced for the band origin of the perturber state and its value for $\omega_e[^{12}C^{16}O](v+\frac{1}{2}) = 370(40)$ cm^{-1}, fitted using the data in Table I, suggests the observed level has a low vibrational excitation, likely with $v = 0$. Taken together, our conclusions on the characterisation of the perturber lead to its assignment as $E''(v = 0)$, as foreshadowed in Sec. III.

There is a large discrepancy in the quantity y between the cases of $^{13}C^{18}O$ and all other isotopologues. $W(1)$ occurs about 30 cm^{-1} higher in energy than expected for $^{13}C^{18}O$ and the perturber is also apparently shifted upwards. This may be a result of an interaction with the nearby lower-lying state responsible for the additional broad feature indicated in Fig. 4. Additionally, the B-values of $W(1)$ and $E''(0)$ in $^{13}C^{18}O$ do not deviate from the expected mass scaling, as indicated by the quantity x in Table I. This suggests that any interaction with the state responsible for the broad feature is of homogeneous character and is consistent with the hypothesis that it arises due to the $v = 5$ level of the $E'\,^1\Pi$ state.

The W state T_e and ω_e values deduced from Table I from the mass dependence of $W(1)$ differ significantly from those known from the complete $W(v = 0{-}3)$ experimental record[1,19] and theory.[27] This discrepancy arises from the large electronic interactions mixing the W state with remote levels of the $E'\,^1\Pi$ state and other Rydberg $^1\Pi$ states, whose perturbing effect is isotopologue dependent.[2]

An estimate of the equilibrium internuclear separation, R_e, of the perturber state may be made from its equilibrium rotational constant, B_e, according to[39]

$$R_e = \sqrt{\frac{\hbar^2}{2\mu B_e}}, \tag{9}$$

giving a value of 3.5 a.u. (1.9 Å), assuming $B_e \approx B_{E''}$ from Table I. This is significantly larger than the equilibrium separation of CO's Rydberg states ($R_e < 2.2$ a.u.) or the valence $E'\,^1\Pi$ state ($R_e \simeq 2.3$ a.u.) which has been shown to interact strongly with $W\,^1\Pi$.[2] Instead, the deduced R_e is in good agreement with an adiabatic $^1\Pi$ potential-well[26] plotted in Fig. 1. We propose that the observed perturber level belongs to the first bound state of this well, to which we choose to assign the spectroscopic label E''. The large-R_e well is formed from the adiabatic interaction of the outer limb of the $E'\,^1\Pi$ diabatic state and a repulsive curve which dissociates to ground state C and O atoms. The curve calculated by Guberman[26] has an equilibrium position with $T_e = 105100$ cm^{-1} and $R_e = 3.60$ a.u., in good agreement with our experimentally deduced values of about 105 300 cm^{-1} and 3.5 a.u. The vibrational constant determined by Guberman,[26] $\omega_e = 492$ cm^{-1}, indicates our isotope-shift-deduced value of $\omega_e[^{12}C^{16}O](v+\frac{1}{2}) = 370(40)$ cm^{-1} is most consistent with the *ab initio* curve when assigning the observed E'' level to $v = 0$, as assumed above.

The same bound state calculated by Guberman[26] also appears in the calculations of Vázquez *et al.*[27] with predicted spectroscopic parameters $T_e = 104640$ cm^{-1} and $R_e = 3.65$ a.u. An earlier calculation[25] led to the suggestion its bound vibrational levels may have appeared in previously recorded emission spectra, which has since been refuted.[40] Lefebvre-Brion and Eidelsberg[2] suggested an indirect influence of the predicted state may arise due to its perturbation of the vibrational energies of the $E'\,^1\Pi$ state, which remains to be verified. The disagreement between the above-noted

ab initio-deduced T_e values and our experimental value is comparable to discrepancies noted with other better-observed states.[25–27]

The overlap of $W(1)$ and $E''(0)$ vibrational wavefunctions is completely negligible because of the large separation of their potential-energy curves. We therefore propose that the observed interaction is mediated by the $E'\,^1\Pi$ state. An experimentally constrained study of $^1\Pi$ Rydberg-valence interactions by Lefebvre-Brion and Eidelsberg[2] found an electronic coupling of about 400 cm^{-1} between the diabatic E' and W states and a 3%–21% admixture of E' electronic character in the observed $W(1)$ level, depending on isotopologue. In their analysis, the degree of admixture is largely dependent on the proximity of the unobserved $E'(5)$ level to $W(1)$, predicted to lie around 40 cm^{-1} higher in energy, but cannot be separated from the influence of other Rydberg states. Additionally, as mentioned above, the E'' potential well is formed from the electronic interaction of a repulsive state and the E' outer limb in a diabatic representation. The minimum separation of adiabatic E' and E'' potential-energy curves in Fig. 1, ≈1100 cm^{-1}, provides an estimate for the magnitude of this interaction, 1100/2 = 550 cm^{-1} (Ref. 39, Sec 3.3). Considering the partial E' electronic character of $W(1)$ and the large coupling of E' with the E''-antecedent repulsive state, our determination of the effective interaction of $W(1)$ and $E''(0)$ of around 5 cm^{-1} is quite plausible. Quantitative modelling of the experimentally deduced interaction would require the solution of a coupled vibrational Schrödinger equation using accurate potential-energy curves for all the states involved.

V. DEPERTURBATION OF INTENSITIES AND WIDTHS

The deperturbation of $W(1)$ and $E''(0)$ energy levels also generated J-dependent state mixing coefficients. Using these, we simulated the intensity borrowing of an intrinsically dark perturber, assuming a J-independent band f-value for $W(1)$. The calculated f-values of $W(1)$ and the perturber are shown in Fig. 6 and the magnitude of transferred intensity is quite satisfactory when compared with the experimental values. The model predicts one or more strong perturber transitions for J above the crossing point which are not observed, most likely because the excited perturber levels are suddenly broadened and indistinguishable in our spectra.

The observed patterns of $W(1)$ linewidths, shown in Fig. 7, were also well reproduced using the mixing coefficients deduced from deperturbing term values. For this, we assumed that both $W(1)$ and the perturber level couple to the dissociation continuum with interaction parameters proportional to the square-root of their predissociation widths, Γ_W and Γ''_E, respectively. These were assumed to be of the form

$$\Gamma_W = a + bJ(J+1) \tag{10}$$

and

$$\Gamma_{E''} = c. \tag{11}$$

TABLE II. Deperturbed predissociation widths of $W(1)$ and the perturber state, $E''(0)$.[a]

	Γ_W	$\Gamma_{E''}$
$^{12}C^{16}O$	1.58(1) + 0.470(5) · $J(J+1)$	5.1(11)
$^{12}C^{17}O$	0.55(42) + 0.018(6) · $J(J+1)$	5.7(39)
$^{12}C^{18}O$	0.75(23) + 0.033(4) · $J(J+1)$	5.7(8)
$^{13}C^{16}O$	0.61(45) + 0.031(6) · $J(J+1)$	7.2(10)
$^{13}C^{18}O$	3.8(20) − 0.007(7) · $J(J+1)$	2.1(47)

[a]In units of cm^{-1}, FWHM and with 1σ uncertainties shown in parentheses in units of the least significant figure.

The parameters a, b, and c, listed in Table II, were obtained from a best fit to the experimental widths of the quantities,

$$\Gamma'_W(J) = [c_{WW}(J)\sqrt{\Gamma_W(J)} - c_{E''W}(J)\sqrt{\Gamma_{E''}(J)}]^2 \tag{12}$$

and

$$\Gamma'_{E''}(J) = [c_{WE''}(J)\sqrt{\Gamma_W(J)} - c_{E''E''}(J)\sqrt{\Gamma_{E''}(J)}]^2. \tag{13}$$

Here, c_{ij} is the coefficient describing the mixing of pure level i into observed level j. The negative sign of the interference in these equations was required to reproduce the correct sense of the interference between W and E'' widths around the level crossing. Actually, the observed interference pattern only constrains the sign of the product of three interactions: $W(1)$ with $E''(0)$, $W(1)$ with the continuum, and $E''(0)$ with the continuum; and other combinations of signs will produce the same width pattern.[41]

The J-independent part of the $W(1)$ predissociation broadening may arise from its electronic coupling to other $^1\Pi$ states and their mutual spin-orbit interaction with further states of $^3\Pi$ symmetry,[2,13,24] a process which has yet to be fully quantified. The assumed J-dependent interaction of $W(1)$ with the continuum in Eq. (10) was necessary to explain the observed trend of $W(1)$ linewidths away from the perturber crossing point. The physical cause of this dependence could be a multichannel effect, whereby many remote $^1\Pi$ and $^3\Pi$ levels influence the width of $W(1)$ in a complicated way. Similar J-dependent widths have been determined experimentally for other $W(v)$ levels[1,4] and a confident explanation of their predissociation mechanism awaits comprehensive modelling of CO's interacting electronic states considering a large set of vibrational levels.[2,16] Alternatively, a simpler J-dependent mechanism may be at work, whereby a rotational interaction proportional to $\sqrt{J(J+1)}$ mixes $W(1)$ with an unbound state of $^1\Sigma$ or $^1\Delta$ symmetry. The $^1\Sigma$ case is ruled out by the parity independence of the observed predissociation broadening; that is, the P- and R-branch widths, and Q-branch widths vary similarly. A possible candidate for rotationally induced predissociation is then mixing of $W(1)$ with the continuum of the $D\,^1\Delta$ state. This state dissociates to ground-state $C(^3P) + O(^3P)$ atoms, and has a principal electronic configuration differing from $W\,^1\Pi$ by only a single electron orbital.[42] Indeed, the product-sensitive photodissociation $^{12}C^{16}O$ experiment of Gao *et al.*[24] found a 75% probability that the $J = 1$ and 2 levels of $W(1)$ dissociate to form ground state atoms, with the remainder dissociating as $C(^1D) + C(^3P)$.

These secondary products correlate with the dissociation energy of triplet-multiplicity molecular states only.

It is not clear from the constraining experimental widths whether the perturber state truly interacts with the continuum independently of J, as assumed in Eq. (11). The deduced interaction is isotopologue independent within the fitting uncertainties of Table II and is quite consistent with the direct predissociation of the $v = 0$ level of the large-R potential well and repulsive state shown in Fig. 1.

VI. SIMILARITY TO N_2

A previous comparison of the electronic states of CO with the isoelectronic molecule N_2 noted the similarity of molecular parameters for some pairs of states and the approximate correspondence of their principal configuration of single-electron molecular orbitals.[13] Significant differences do however occur because of the lack of *gerade/ungerade* symmetry in the case of CO and the differing orbital and spin angular momenta of the separated atoms.

As noted by Lefebvre-Brion and Lewis,[13] the $W\,^1\Pi$ state of CO studied here is configurationally analogous to the $o_3\,^1\Pi_u$ state of N_2, with both attributable to a $3s\sigma$ electron orbiting an excited $^2\Pi$ (or $^2\Pi_u$) ionic core. They further compared the $b\,^1\Pi_u$ state of N_2 with a posited CO state $E'\,^1\Pi$, which was later observed[2] and is approximately isoconfigurational with $b\,^1\Pi_u$ at its calculated potential minimum.[27]

A comparison of $^1\Pi$ (or $^1\Pi_u$) potential-energy curves calculated by Guberman for N_2[43] and CO[26] indicates a further correspondence of the outer-well of the $b\,^1\Pi_u$ states with the $E''\,^1\Pi$ state studied in this paper. That is, a diabatic linear combination of E' and E'' states results in a single bound potential, analogous to the $b\,^1\Pi_u$ state, crossed near 3.3 a.u. by a repulsive curve which dissociates to ground state $C(^3P)$ and $O(^3P)$ atoms. However, no corresponding $^1\Pi_u$ state capable of perturbing $b\,^1\Pi_u$ in N_2 can be constructed from a pair of ^4S ground-state N atoms.

VII. CONCLUSION

The photoabsorption spectrum of $W(1) \leftarrow X(0)$ was recorded for five isotopologues of CO and rotationally analysed, revealing a perturbation influencing its line positions and their predissociative broadening, as well as the appearance of extra lines from a previously unobserved level. A complete listing of these data is provided in the supplementary material.[37]

We were able to deperturb the observed levels and attain spectroscopic constants for the perturbing level by combining information from all isotopologues. The deduced equilibrium internuclear distance of the perturbing state and isotopic shifts of its energy levels is not consistent with the well-known Rydberg and valence states of CO. Instead, we assign the perturbing level to the $v = 0$ level of a hitherto unobserved $^1\Pi$ state predicted in *ab initio* calculations at large internuclear distance, which we choose to label E''.

The rapid J-dependence of $W(1)$ predissociation broadening around the crossing point with the new $E''(0)$ level is the result of interference between their separate interactions with the dissociation continuum. Deperturbing this interaction required a rotational dependence for the deperturbed predissociation of $W(1)$, suggesting multiple predissociation pathways are available to $W(1)$. Further exploration of this phenomenon would benefit from an extension of this deperturbation to include, potentially, several other interacting electronic states including those of Σ symmetry or triplet multiplicity. We intend to further study CO's excited states experimentally in order to help constrain such a deperturbation.

ACKNOWLEDGMENTS

We wish to thank H. Lefebvre-Brion for very useful discussions and helpful suggestions. A.H. was supported by Grant No. 648.000.002 from the Netherlands Organisation for Scientific Research (NWO) via the Dutch Astrochemistry Network. This research was supported by funds from National Aeronautics and Space Administration (NASA) (Grant Nos. NNX09AC5GG to Wellesley College and NNG 06-GG70G and NNX10AD80G to the University of Toledo), CNRS (France), and Programme National Physico-Chimie du Milieu Interstellaire (PCMI). L.G. and J.L.L. acknowledge the financial support of the European Community 7th Framework Programme (FP7/2007-2013) Marie Curie ITN under Grant Agreement # 238258.

[1] M. Eidelsberg, J. L. Lemaire, S. R. Federman, G. Stark, A. N. Heays, Y. Sheffer, L. Gavilan, J.-H. Fillion, F. Rostas, J. R. Lyons, P. L. Smith, N. de Oliveira, D. Joyeux, M. Roudjane, and L. Nahon, Astron. Astrophys. **543**, A69 (2012).
[2] H. Lefebvre-Brion and M. Eidelsberg, J. Mol. Spectrosc. **271**, 59 (2012).
[3] L. Gavilan, J. L. Lemaire, M. Eidelsberg, S. R. Federman, G. Stark, A. N. Heays, J.-H. Fillion, J. R. Lyons, and N. de Oliveira, J. Phys. Chem. A **117**, 9644 (2013).
[4] M. Eidelsberg, J. L. Lemaire, S. R. Federman, G. Stark, A. N. Heays, L. Gavilan, J. R. Lyons, P. L. Smith, N. de Oliveira, and D. Joyeux, Astron. Astrophys. **566**, A96 (2014).
[5] G. Stark, A. N. Heays, J. R. Lyons, P. L. Smith, M. Eidelsberg, S. R. Federman, J. L. Lemaire, L. Gavilan, N. de Oliveira, D. Joyeux, and L. Nahon, Astrophys. J. **788**, 67 (2014).
[6] R. Visser, E. F. van Dishoeck, and J. H. Black, Astron. Astrophys. **503**, 323 (2009).
[7] A. G. G. M. Tielens, Rev. Mod. Phys. **85**, 1021 (2013).
[8] M. Eidelsberg and F. Rostas, Astrophys. J. Suppl. Ser. **145**, 89 (2003).
[9] J. Lyons and E. Young, Nature (London) **435**, 317 (2005).
[10] A. N. Heays, R. Visser, R. Gredel, W. Ubachs, B. R. Lewis, S. T. Gibson, and E. F. van Dishoeck, Astron. Astrophys. **562**, A61 (2014).
[11] W.-Ü. L. Tchang-Brillet, P. Julienne, J. Robbe, C. Letzelter, and F. Rostas, J. Chem. Phys. **96**, 6735 (1992).
[12] M. Eidelsberg, F. Launay, K. Ito, T. Matsui, P. Hinnen, E. Reinhold, W. Ubachs, and K. Huber, J. Chem. Phys. **121**, 292 (2004).
[13] H. Lefebvre-Brion and B. R. Lewis, Mol. Phys. **105**, 1625 (2007).
[14] W. Ubachs, I. Velchev, and P. Cacciani, J. Chem. Phys. **113**, 547 (2000).
[15] J. Baker and F. Launay, J. Chem. Phys. **123**, 234302 (2005).
[16] M. Majumder, N. Sathyamurthy, G. J. Vázquez, and H. Lefebvre-Brion, J. Chem. Phys. **140**, 164303 (2014).
[17] C. Letzelter, M. Eidelsberg, F. Rostas, J. Breton, and B. Thieblemont, Chem. Phys. **114**, 273 (1987).
[18] G. Stark, K. Yoshino, P. Smith, K. Ito, and W. Parkinson, Astrophys. J. **369**, 574 (1991).
[19] M. Eidelsberg and F. Rostas, Astron. Astrophys. **235**, 472 (1990).
[20] M. Eidelsberg, Y. Viala, F. Rostas, and J. J. Benayoun, Astron. Astrophys. Suppl. Ser. **90**, 231 (1991).
[21] M. Eidelsberg, J. Benayoun, Y. Viala, F. Rostas, P. Smith, K. Yoshino, G. Stark, and C. Shettle, Astron. Astrophys. **265**, 839 (1992).

[22]P. Hinnen, S. Stolte, W. Hogervorst, and W. Ubachs, J. Opt. Soc. Am. B **15**, 2620 (1998).
[23]M. Eidelsberg, Y. Sheffer, S. R. Federman, J. L. Lemaire, J. H. Fillion, F. Rostas, and J. Ruiz, Astrophys. J. **647**, 1543 (2006).
[24]H. Gao, Y. Song, Y.-C. Chang, X. Shi, Q.-Z. Yin, R. C. Wiens, W. M. Jackson, and C. Y. Ng, J. Phys. Chem. A **117**, 6185 (2013).
[25]S. V. O'Neil and H. F. Schaefer, J. Chem. Phys. **53**, 3994 (1970).
[26]S. L. Guberman, J. Phys. Chem. A **117**, 9704 (2013).
[27]G. J. Vázquez, J. M. Amero, H. P. Liebermann, and H. Lefebvre-Brion, J. Phys. Chem. A **113**, 13395 (2009).
[28]N. de Oliveira, D. Joyeux, D. Phalippou, J.-C. Rodier, F. Polack, M. Vervloet, and L. Nahon, Rev. Sci. Instrum. **80**, 043101 (2009).
[29]N. de Oliveira, M. Roudjane, D. Joyeux, D. Phalippou, J.-C. Rodier, and L. Nahon, Nat. Photon. **5**, 149 (2011).
[30]L. Nahon, N. de Oliveira, G. A. Garcia, J.-F. Gil, B. Pilette, O. Marcouille, B. Lagarde, and F. Polack, J. Synchrotron Radiat. **19**, 508 (2012).
[31]G. Stark, B. R. Lewis, S. T. Gibson, and J. P. England, Astrophys. J. **520**, 732 (1999).
[32]S. R. Federman, M. Fritts, S. Cheng, K. M. Menningen, D. C. Knauth, and K. Fulk, Astrophys. J. Suppl. Ser. **134**, 133 (2001).
[33]A. N. Heays, G. D. Dickenson, E. J. Salumbides, N. de Oliveira, D. Joyeux, L. Nahon, B. R. Lewis, and W. Ubachs, J. Chem. Phys. **135**, 244301 (2011).
[34]G. Herzberg, *Molecular Spectra and Molecular Structure I: Spectra of Diatomic Molecules*, 2nd ed. (Krieger Publishing Company, 1989).
[35]P. F. Levelt and W. Ubachs, Chem. Phys. **163**, 263 (1992).
[36]J. A. Coxon and P. G. Hajigeorgiou, J. Chem. Phys. **121**, 2992 (2004).
[37]See supplementary material at http://dx.doi.org/10.1063/1.4897326 for experimental line energies, strengths, and widths; and derived quantities.
[38]K. P. Huber and G. Herzberg, *Molecular Spectra and Molecular Structure IV: Constants of Diatomic Molecules* (Van Nostrand, New York, 1979).
[39]H. Lefebvre-Brion and R. W. Field, *The Spectra and Dynamics of Diatomic Molecules* (Elsevier, Amsterdam, 2004).
[40]S. Tilford and J. Simmons, J. Mol. Spectrosc. **53**, 436 (1974).
[41]S. Kasahara, M. Shibata, M. Baba, and H. Katô, J. Phys. Chem. A **101**, 422 (1997).
[42]M. E. Rosenkrantz and K. Kirby, J. Chem. Phys. **90**, 6528 (1989).
[43]S. L. Guberman, J. Chem. Phys. **137**, 074309 (2012).